



Investigation of Surface Integrity Up-Milling Magnesium Oxide Particle Reinforced Wood-Based Composite

Jinxin Wang¹ · Rongsheng Jiang¹ · Zhanwen Wu¹ · Zhaolong Zhu² · Longzhi Yang³ · Pingxiang Cao¹

Received: 12 March 2021 / Revised: 12 September 2022 / Accepted: 12 October 2022 / Published online: 4 January 2023
© The Author(s), under exclusive licence to Korean Society for Precision Engineering 2022

Abstract

Metal oxide reinforced composite, as a new kind of engineering material, was an essential research topic to industry. Magnesium oxide as particle-reinforced phase, were mixed with wood fiber-matrix to enhance the mechanical properties of composite. However, the research on the surface quality of this composite is still desirable for expanding its application. In order to investigate the surface integrity of this kind particle-reinforced wood-based composite, spiral up-milling experiments were performed with different cutting depth and cutting speed. The effect of cutting speed and cutting depth on surface integrity was investigated. According to the calculation results of black pixels proportion of binary image of machined surface, surface defects were greatly affected by cutting depth rather than cutting speed. Defects, such as pile-up and debonding of particles, were usually observed under 0.5 mm cutting depth, meanwhile, extensive damage of flaking and fracture of wood fiber-matrix were usually observed under 1.5 mm cutting depth. In all, the machined surface formation mechanism of this composite can be different by changing cutting depth.

Keywords Magnesium oxide particle-reinforced · Cutting depth · Cutting speed · Material removal rate · Surface formation mechanism

1 Introduction

Wood-based materials, as a kind of environmental protection biomass material [1], were widely applied in furnishings field, such as doors and windows, fencing and flooring in terms of their flame retardancy, moisture resistance, insect prevention and so on properties [2–8]. However, for the applications in engineering field, metal-matrix composites are still mainly used due to its high hardness, stiffness, specific strength and low thermal expansion [9]. In order to expand the application of wood-based materials in engineering industry, magnesium oxide particle reinforced wood fiber-matrix composite has emerged, which inspired by a

founding that claims particle-reinforced composites have advantage of easy manufacturing and low cost [10].

Magnesium oxide particle belongs to one kind of ceramic materials. It is difficult to cut ceramic materials due to its high hardness, leading to machine problems in surface quality [11–13]. Therefore, surface integrity of magnesium oxide particle reinforced wood fiber-matrix composite is still desired to investigate for expanding its application [14].

A series of surface integrity of particle-reinforced metal matrix composites was in focus by many researchers. Surface integrity of Silicon nitride particle-reinforced aluminium alloy using PCD tools was investigated through scanning electron microscope, it is concluded that the defect of machined surface made form particle-reinforced were mainly voids, scales, and scratches. In addition, an affected surface layer with a thickness of about 20–35 μm was also observed [15]. Cutting mechanism and damage behavior of particle-reinforced composites was studied by Yu, they found the failure mode and mechanism of machined surface [16]. Above studies, surface formation mechanism of particle-reinforced metal matrix composites is quite clearly. However, the surface formation about particle-reinforced

✉ Pingxiang Cao
njfucpx@163.com

¹ College of Materials Science and Engineering, Nanjing Forestry University, No. 159 Longpan Road, Nanjing, Jiangsu, China

² College of Furnishings and Industrial Design, Nanjing Forestry University, Nanjing, China

³ Department of Computer and Information Sciences, Northumbria University, Newcastle upon Tyne, UK

wood-based composites was not clear, because the anisotropy of wood is compared to the isotropy of metal.

The effect of cutting parameters on surface quality still need to be addressed [17–19]. Silicon nitride particle-reinforced aluminium alloy machined by PCD tools in high-speed milling was investigated. Their results show that an increased cutting speed as well as feed rate can lead to a severe surface defect. It is also concluded that different superimposed effects, comprising particle pull-out as well as the subsurface voids within the surface layer results in the formation of deep voids [20]. The influence of cutting speed, feed per tooth and cutting depth on surface roughness of machined surface has been investigated. They founded that an increased feed per tooth and a decreased cutting speed led to an increasing surface roughness [21]. The optimal cutting parameters of cutting speed, feed and cutting depth when machining aluminium silicon carbide particulate metal matrix composite were investigated, they found cutting speed and cutting depth have the most contribution to cutting [22]. Although above studies concluded cutting speed and cutting depth have significant influence on surface integrity, the surface formation mechanism of under these cutting parameters still need to be revealed.

As mentioned above, surface quality of particle-reinforced composites has been investigated a lot, and applied in many engineering fields. But until now, as a new kind composite, MgO-particle-reinforced wood fiber-matrix composite, there is still no research about the machinability of this composite. In order to expand its application in engineering materials, it is desirable to investigate its surface integrity under different cutting conditions.

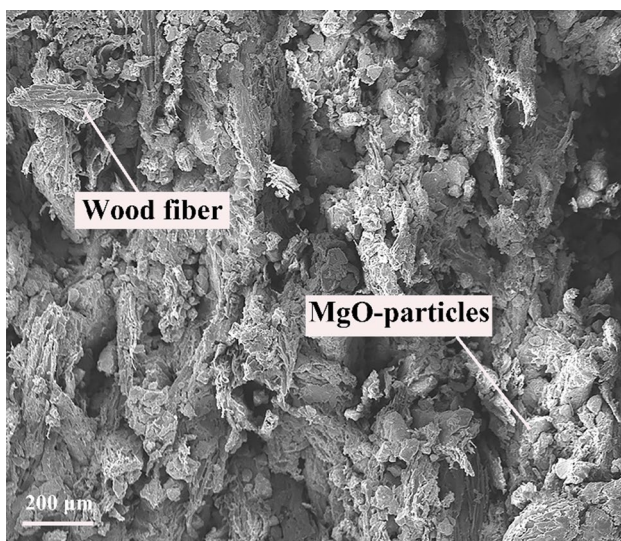


Fig. 1 SEM image of MgO-particle-reinforced wood fiber-matrix composite

In this experimental study, particle-reinforced wood-based composite was selected as objective. Spiral up-milling tests were carried out to investigate surface formation mechanism using PCD tool. Surface defects were determined by images of scanning electronic microscope.

2 Material and Methods

2.1 Materials

MgO-particle-reinforced wood fiber-matrix composite, was used as milling object in this study. The raw material was supplied by HOMAG China Golden Field Ltd., China. The workpieces were rectangular blocks of 140 mm × 80 mm × 7 mm (length × width × thickness), which contained 55.0 wt.% wood fiber, 36.8 wt.% MgO, and 2.3 wt.% SiO₂, as well as 5.9 wt.% some additives such as pigments. A representative microstructure of MgO-particle-reinforced wood fiber-matrix composite is shown in Fig. 1. Physical and mechanical properties of the workpieces are listed in Table 1.

In this experiment, the helix milling cutter with helix angle of 70°. The diameter of the tool with six cutting teeth was 140 mm. The blades were fabricated by injection moulding at high temperature (Kyocera Group Co. Ltd. Japan). Table 2 provide the tool parameters and mechanical properties of the cutting tools used in this study.

2.2 Experimental Set-up

Experimental set-up of machinability studies of MgO-particle-reinforced wood fiber-matrix composite was presented in

Table 1 Workpiece properties of MgO-particle-reinforced wood fiber-matrix composite

Density (g/cm ³)	Modulus of rupture (MPa)	Modulus of elasticity (MPa)	Impact strength (KJ/m ²)	Thickness swelling (%)
1.25	18.5	4.79×10^3	22	1.5

Table 2 Tool geometry and mechanical properties of PCD

Helix angle (°)	70
Rake angle (°)	10
Clearance angle (°)	8
Diameter (mm)	140
Number of teeth	6
Modulus of elasticity (Gpa)	800
Thermal conductivity (W·m ⁻¹ ·K ⁻¹)	560
Hardness (HV)	8000

Fig. 1. Spiral up-milling tests were performed on a MGK01 four-axis CNC machining center in Fig. 2a. As shown in Fig. 2b, dynamic cutting forces were monitored by a dynamometer (Kistler 9257B, Switzerland) with a charge amplifier (5070A, Switzerland) during the milling process. The sampling frequency of the recorder was less than the natural frequency of 3.5 kHz. Cutting force components in three orthogonal directions were measured. (Fig. 2b). The average resultant cutting force F_r was calculated from cutting force components in X, Y, and Z directions using the formula (1). A surface profiler was used to measure the surface roughness R_a , and the ACCTee software was used to calculate the surface roughness in Fig. 2c. The cut-off and sampling length were determined as 0.8 mm and 10 mm in this work. A scanning electronic microscope (SEM) was used to observe the machined surface topography.

$$F_r = \sqrt{(F_x)^2 + (F_y)^2 + (F_z)^2} \tag{1}$$

2.3 Calculation of Material Removal Rate and Experimental Design

In spiral up-milling, the cutting width b is periodically varying compared with a fixed cutting width in cylindrical milling. When the tooth of cutter just cut into the workpiece, b is very small, then gradually increases to the maximum, and finally decreases as tooth cut out. Figure 3 shows a schematic of chip section in spiral up-milling.

For one tooth, the unit width of chip is:

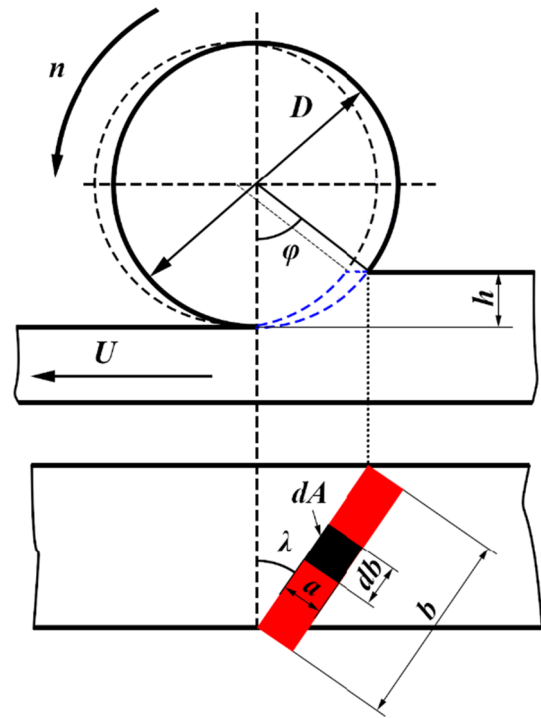
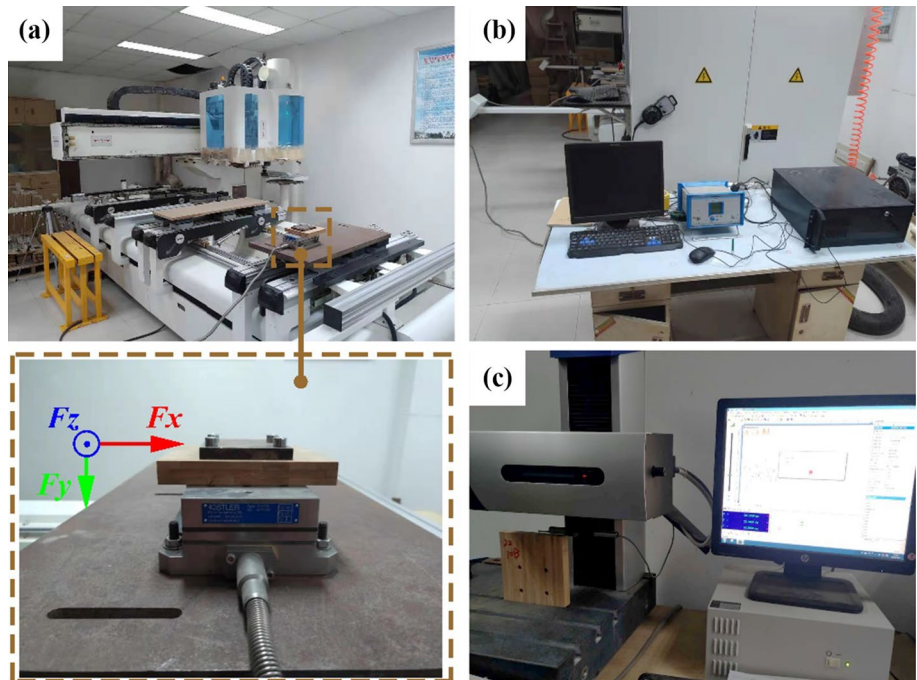


Fig. 3 Schematic of chip volume in spiral cutting

$$db = \frac{D}{2} \frac{d\phi}{\sin \lambda} = \frac{D}{2 \sin \lambda} d\phi \tag{2}$$

where b is cutting width (mm), ϕ is the contact angle between the cutter and workpiece ($^\circ$), λ is the spiral angle ($^\circ$), D is the diameter of tool (mm).

Fig. 2 Experimental set-up: a machine center; b amplifier connected to PC; c surface profiler



Integral of db , the width of chip is:

$$b = \int_0^\varphi \frac{D}{2 \sin \lambda} d\varphi = \frac{D \cdot \varphi}{2 \sin \lambda} \tag{3}$$

For infinitesimal elements, the unit cross-section area (dA) of the chips cut by the length of cutter teeth can be expressed as:

$$dA = a \cdot db = U_z \cdot \sin \varphi \cdot \frac{D \cdot d\varphi}{2 \sin \lambda} = \frac{D \cdot U_z}{2 \sin \lambda} \cdot \sin \varphi \cdot d\varphi \tag{4}$$

where a is chip thickness (mm), U_z is feed per tooth (mm/Z).

The cross-sectional area of chips cut by one tooth is:

$$A = \int_0^\varphi \frac{D \cdot U_z}{2 \sin \lambda} \cdot \sin \varphi \cdot d\varphi = \frac{D \cdot U_z}{2 \sin \lambda} (1 - \cos \varphi) \tag{5}$$

The volume of chip cut per tooth is:

$$V = A \cdot \int_0^\varphi \frac{D}{2} \cdot d\varphi = \frac{D^2 \cdot U_z}{4 \sin \lambda} \cdot \varphi (1 - \cos \varphi) \tag{6}$$

The relation between contact angle, cutting depth and diameter of the tool is as follows:

$$\cos \varphi = 1 - \frac{2h}{D} \tag{7}$$

where the h is the cutting depth (mm).

Bring formula (7) into formula (6), the material removal rate is:

$$\begin{aligned} MRR &= \frac{V \cdot U}{U_z} = \frac{D^2 \cdot U}{4 \sin \lambda} \cdot \varphi (1 - \cos \varphi) \\ &= \frac{D \cdot U \cdot h}{2 \sin \lambda} \cdot \arccos \left(1 - \frac{2h}{D} \right) \end{aligned} \tag{8}$$

where MRR is the material removal rate (mm³/s), U is the feed rate (mm/s).

In this work, different cutting speed and cutting depth with a constant feed rate were set as cutting parameters. The detailed experimental design for the research into the effect of cutting speed and cutting depth on cutting force and surface roughness is summarized in Table 3. It is clearly to be found that MRR has nothing to do with cutting speed according to formula (8).

3 Results and Discussion

3.1 Analysis of Cutting Force

3.1.1 Effect of Cutting Parameters on Resultant Cutting Force

Figure 4 shows the trend of cutting force components as time increased. The first 0.25 s corresponded to a transient

process before reaching the steady state cutting process. Following the approximately 1.5 s was the stable cutting process. After this, the tool was disengaged. An average of resultant cutting force during stable cutting process was calculated after filtered, and it was used for further analysis.

Figure 5 shows the influences of cutting speed and cutting depth on resultant cutting force. Resultant cutting force decreased with the increase of cutting speed and increased with the increase of cutting depth. At the same cutting depth, when the cutting speed increased from 35 to 45 m/s, the resultant cutting force decreased about 10 N, 17 N and 45 N, respectively. However, at the same cutting speed, when the cutting depth increased from 0.5 to 1.5 mm, the resultant cutting force correspondingly increased by about 187 N, 152 N and 151 N. It can be easily concluded that the response of cutting depth to cutting force is higher than that of cutting speed in this experiment (at least in the investigated range of parameters). The growth of the resultant cutting force as cutting depth increases is likely related to the increase of MRR . The increase of cutting speed indicates the increase of spindle speed which leads to a lower feed per tooth, resulting in a lower resultant cutting force. In addition, Fig. 5 also shows the standard deviation of the resultant cutting force during each test (see the error bars). The increase of the standard deviation at large cutting depth ($h = 1.5$ mm) clearly indicates the occurrence of cutting force fluctuation.

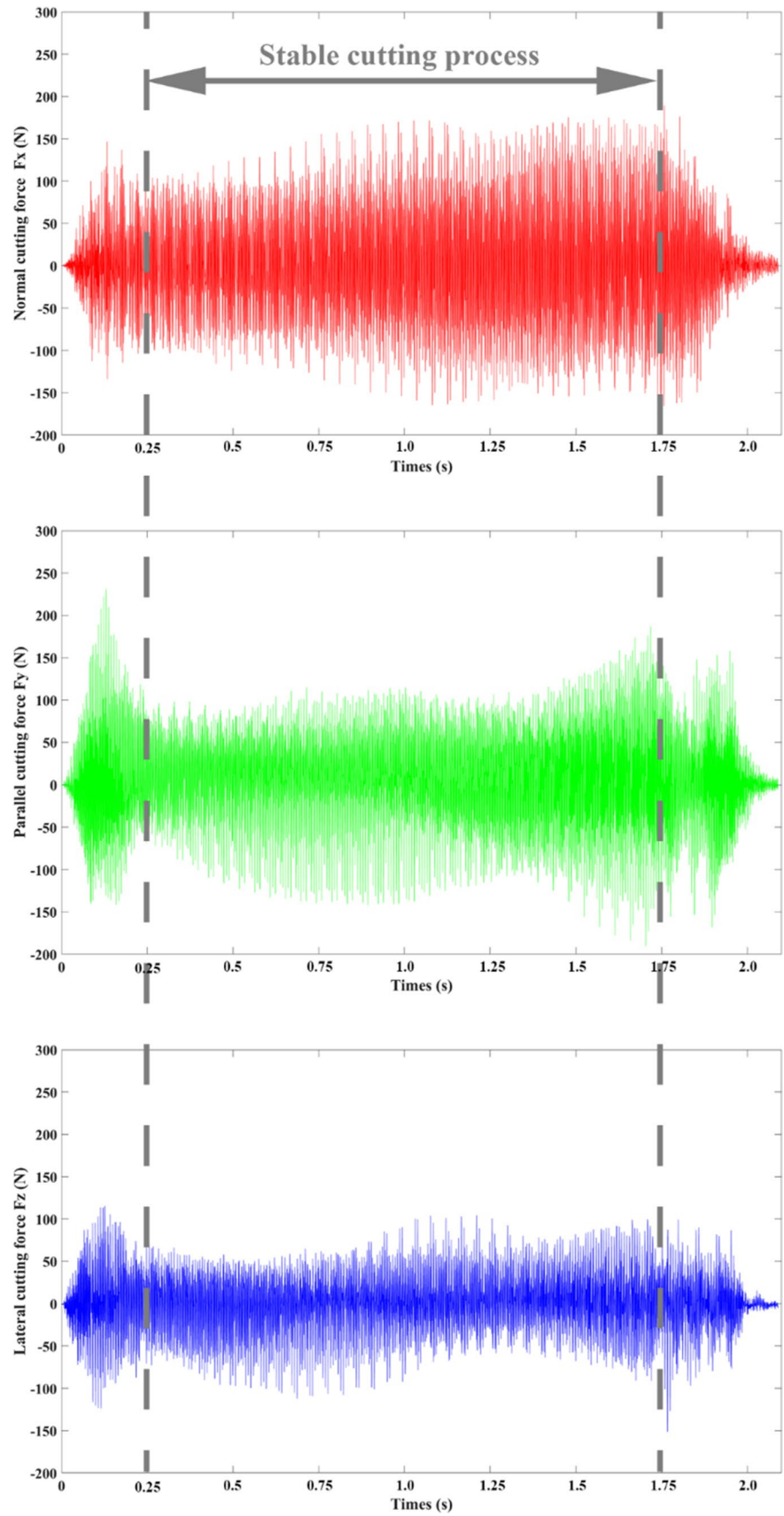
3.1.2 Effect of Cutting Parameters on MRR

According to the Eq. (8), it is found that the MRR is a function of U , λ and h . But only cutting depth and cutting speed were investigated in this work. Therefore, the MRR is dependent of the cutting depth in this study. The characteristic of the MRR as a function of the cutting depth is shown in Fig. 6. The MRR firstly showed a slight upward trend as the cutting depth increased. When the continues increase in cutting depth, the MRR characteristic can be approximated by a linear function in the range of cutting

Table 3 Parameters and levels of spiral up-milling test

Exp. no	Cutting speed (m/s)	Cutting depth (mm)	Feed rate (mm/s)	MRR (mm ³ /s)
1	35	0.5	66.67	297.0
2	35	1.0	66.67	840.4
3	35	1.5	66.67	1545.0
4	40	0.5	66.67	297.0
5	40	1.0	66.67	840.4
6	40	1.5	66.67	1545.0
7	45	0.5	66.67	297.0
8	45	1.0	66.67	840.4
9	45	1.5	66.67	1545.0

Fig. 4 Typical cutting forced components in spiral up-milling



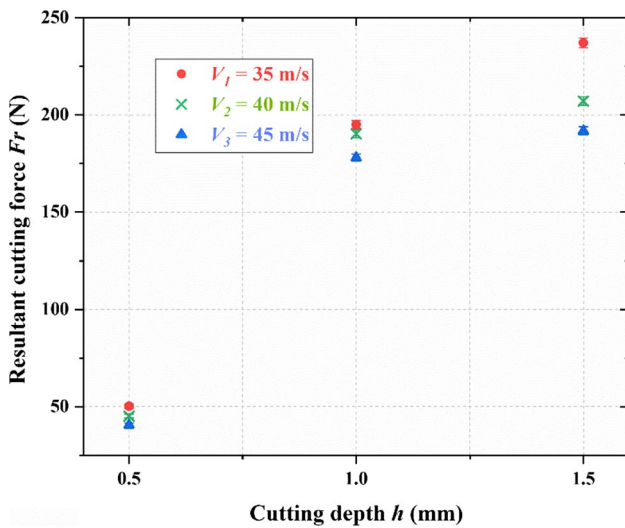


Fig. 5 Comparison of the resultant cutting force for various machining conditions

depth ($0.5 \text{ mm} < h < 1.5 \text{ mm}$). This linear tendency of MRR confirmed the increasing resultant cutting force as the cutting depth increased.

3.2 Analysis of Surface Quality

3.2.1 Effect of Cutting Parameters on Surface Roughness

The influence of cutting speed and cutting depth on surface roughness can be seen in Fig. 7. It is remarkable that there is a similar tendency of the resultant cutting force as the cutting depth increases. Also, machined surface roughness decreased with the increase of cutting speed at the same cutting depth. The difference “L” in Fig. 7 illustrates

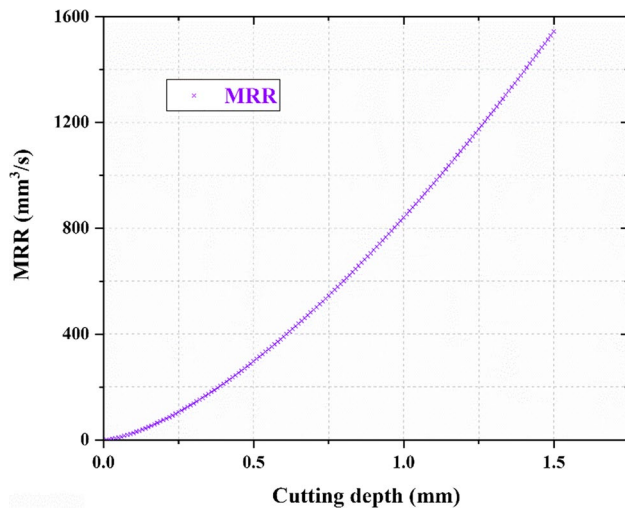


Fig. 6 Material removal rate as a function of the cutting depth

that the machining efficiency can be improved by increasing both cutting depth and cutting speed, while a better surface roughness is obtained. It is of practical significance to improve the machining efficiency of materials for machining industry. Furthermore, if energy consumption is considered, the slight loss of surface roughness can be accepted by reducing the cutting speed. Because the surface roughness of V_2 was close to V_3 .

According to Figs. 5 and 7, the cutting speed had moderate effect on the resultant cutting force and surface roughness (at least in the investigated range of parameters), while the effect of cutting depth was more significant. And it is likely the different behaviors of materials deformation in cutting area in front of the tool tip under different cutting depths. Therefore, the cutting speed $V_2 = 40 \text{ m/s}$ was selected for further analysis of surface topography at the cutting depth of 0.5 mm and 1.5 mm were observed to conjecture the behavior of materials deformation.

3.2.2 Binary Image Analysis of Surface Defects

In order to test the defect rate of machined surface, a viable method of particles size determination using binary image analysis was reported [23]. Specifically, this analysis mainly went through three stages in Fig. 8, including sample image loading, image binarization, and image morphological operation. At stage of images binarization, the threshold value was determined by the “graythresh” function to access the best possible threshold value for each image using MATLAB software. At the stage of morphological operation, image erosion was used to filter the binary image. By

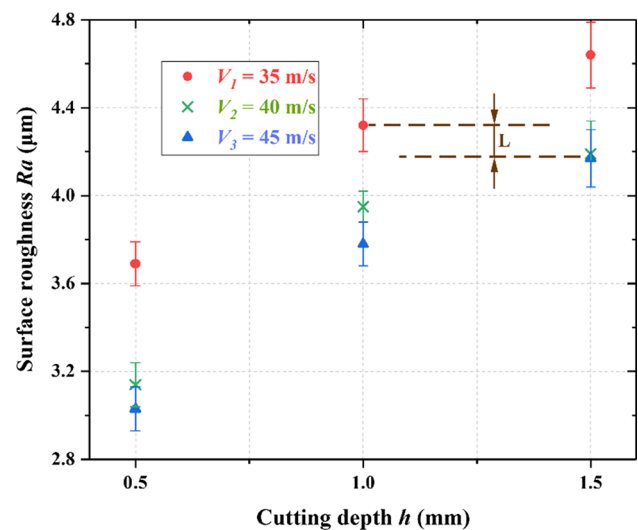


Fig. 7 Comparison of surface roughness for various machining conditions

creating structural elements similar to the shape of defects on the machined surface, the defects are represented by black pixels and others are represented by white pixels.

Figure 9a, b show the binarized image of machined surface under 0.5 mm cutting depth and 1.5 mm cutting depth, respectively. The defect rate of the machined surface was obtained by calculating the proportion of black pixels in the image. According to the calculation results, the defect rates of 0.5 mm cutting depth and 1.5 mm cutting depth are 1.09% and 11.34%, respectively. It can be clearly seen that the proportion of black pixels in image 9(a) was much more than that of image 9(b). It is also confirmed that the surface damage degree of machined surface under 1.5 mm cutting depth is far greater than that under 0.5 mm cutting depth. In other words, when the tool is at the same speed and time

conditions, a depth of cut condition of 1.5 mm can result in far more material breakage in front of the tool tip than at a depth of cut of 0.5 mm. This is because the greater the depth of cut, the more material needs to be removed under the same conditions. Therefore, the degree of material deformation in front of the tool tip goes from mild to severe as the cutting depth increases.

3.2.3 Surface Defects

Camera photos were taken account to evaluate the machined surface integrity in Fig. 10a, d. Some visible defects were observed in Fig. 10d, while Fig. 10a was not. It is no doubt that there is a quite different morphology of machined surface. To further explore this difference, a scanning electronic

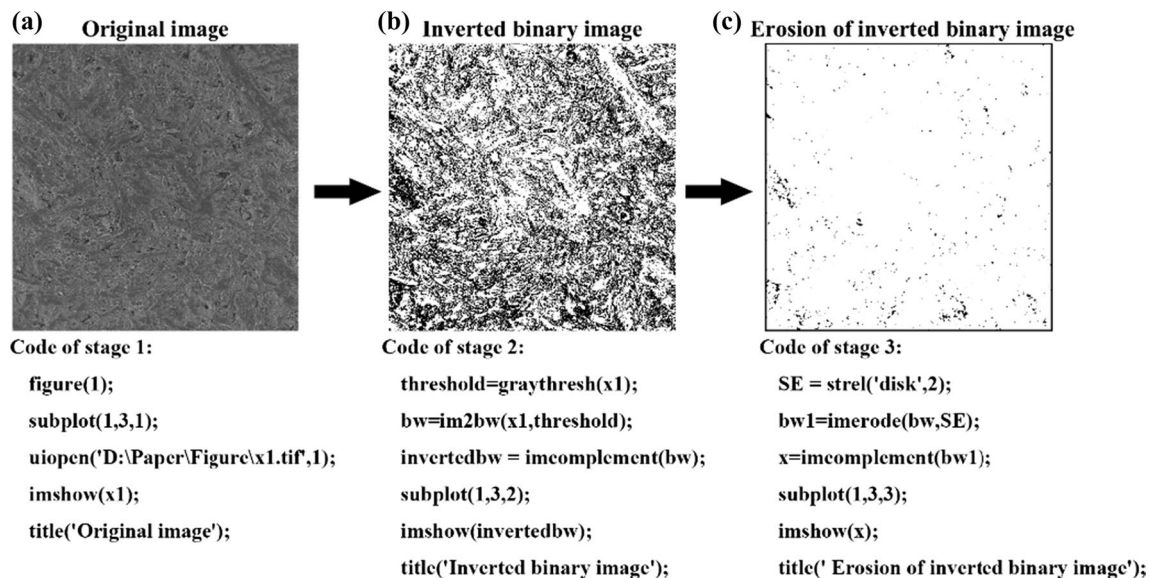
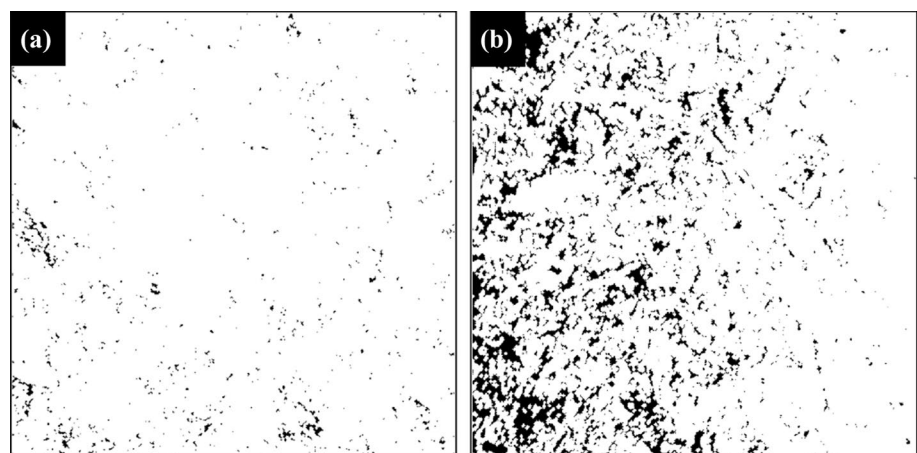


Fig. 8 An example of image analysis. **a** Original image; **b** Inverted binary image (threshold value calculated by the “graythresh” function); **c** Erosion of inverted binary image (disk radius $R=2$)

Fig. 9 Binary image after morphological operations of erosion (disk radius $R=2$). **a** 1.09% defect rate at 0.5 mm cutting depth; **b** 11.34% defect rate at 1.5 mm cutting depth



microscope (SEM) was utilized to assess the topography of machined surface (Fig. 10b, c, e, f). Defects, i.e., crack, pile-up and pits were observed on the machined surface at the cutting depth of 0.5 mm in Fig. 10b, c. In comparison to wood fiber composites without the addition of MgO particles, it has been noted that at small depths of cut, the damage to the machined surface is mainly due to debonding of the wood fibers from the matrix [24]. The formation mechanism of machined surface can be explained as follows. When MgO particles are added, a certain degree of cutting force pushes the hard MgO particles partially into the relatively soft wood matrix, causing cracks and pile-up on the machined surface, as well as pushing the MgO particles partially out of the wood matrix, causing the MgO particles to debond, resulting in pits of the machined surface. This kind of material deformation, however, is implicitly characterized by plastic deformation, such as good re-formability, leading to a lower surface roughness and a higher surface quality.

By contrast, fracture of fibers and extensive flaking of wood fiber layers were observed on the machined surface at the cutting depth of 1.5 mm in Fig. 10e, f. When the cutting depth increased from 0.5 to 1.5 mm, the MRR increased from 297 to 1545 mm³/s. Namely, the volume of material removed in unit time under 1.5 mm cutting depth is about five times of that under 0.5 mm cutting depth. This sharp increase of material removal volume caused a higher resultant cutting force, which enough to tear wood fibers. Besides, wood fibers are not oriented, therefore, flaking of wood fibers was often observed when the wood fibers orientation is similar to the cutting direction. Otherwise, wood fibers fracture was often observed Fig. 10d. At large cutting depth, the addition of MgO has little effect on machined surface damage, as the larger cutting forces cause direct damage to the wood fiber matrix. This also indicates that at large cutting depths, the deformation

behavior of the material tends towards brittle fracture, leading to severe surface damage.

4 Conclusion

In this paper, the surface integrity of MgO-particle-reinforced wood fiber-matrix composite during spiral up-milling was investigated. There are some results can be concluded as follows.

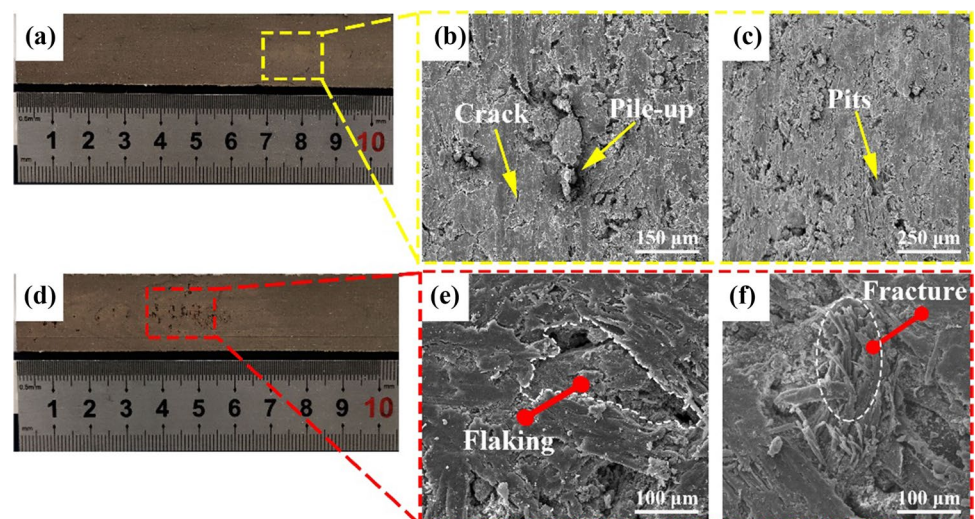
Surface integrity is significantly to be affected by cutting depth than by cutting speed. This is mainly because the MMR increases dramatically when the depth of cut is varied.

At different cutting depths, the deformation of the material in the cutting zone in front of tool tip is closely related to the surface integrity of the machined surface. At small cutting depths, the deformation is characterized by plastic deformation, which results in minor surface defects and better surface quality due to better re-formability. At large depths of cut, on the other hand, the deformation of the material tends to fracture, leading to severe surface damage and poorer machining quality.

Acknowledgements This work is a Project Funded by the National First-class Disciplines (PNFD). The authors are grateful for the support from the National Science Foundation of China (31971594), Leitz Tooling System Co. Ltd. for supplying the samples of PCD tools, and Guofeng Wood Plastic Composite Co. Ltd. for supplying the samples of wood fiber/polyethylene composite.

Author Contributions JW: laboratory experiment, data collection, analysis and discussion of the data, and editing the paper. RJ: project administration, experiment design, analysis and discussion of the data, and writing the paper. ZW: laboratory experiment, data collection and review the paper. ZZ: laboratory experiment, data collection and supervising the work. LY: discussion of the data, and editing the paper. PC: experiment design, laboratory experiment and supervising the work.

Fig. 10 **a** Camera photos of machined surface at the cutting speed $V_2=40$ m/s and cutting depth $h=0.5$ mm; **b** and **c** Defects of machined surface under the condition of (a); **d** Camera photos of machined surface at the cutting speed $V_2=40$ m/s and cutting depth $h=1.5$ mm; **e** and **f** Defects of machined surface under the condition of (d)



Funding This work is a Project Funded by the National First-class Disciplines (PNFD). The authors are grateful for the support from the National Science Foundation of China (31971594).

Availability of data and materials The datasets generated and analysed during the current study are available from the corresponding author on reasonable request.

Declarations

Conflicts of interest The authors declare that they have no conflict of interest.

References

- Kilinc, K., Kanbur, Y., & Tayfun, U. (2019). Mechanical, thermo-mechanical and water uptake performance of wood flour filled polyurethane elastomer eco-composites: Influence of surface treatment of wood flour. *Holzforschung*, 73, 401–407.
- Huang, L. L., Wang, H. Y., Guo, X. L., Jiang, Z. H., Xing, F., Huang, L. L., & Ekevad, M. (2018). Study on continuous cold-pressing technology of engineered wood flooring with EPI adhesive. *Wood Res-Slovakia*, 63, 335–342.
- Bazant, P., Munster, L., Machovsky, M., Sedlak, J., Pastorek, M., Kozakova, Z., & Kuritka, I. (2014). Wood flour modified by hierarchical Ag/ZnO as potential filler, for wood-plastic composites with enhanced surface antibacterial performance. *Industrial Crops and Products*, 62, 179–187.
- Pelaez-Samaniego, M. R., Yadama, V., Lowell, E., & Espinoza-Herrera, R. (2013). A review of wood thermal pretreatments to improve wood composite properties. *Wood Science and Technology*, 47, 1285–1319.
- Lin, Z. Y., & Renneckar, S. (2011). Nanocomposite-based lignocellulosic fibers 2: Layer-by-layer modification of wood fibers for reinforcement in thermoplastic composites. *Composites Part A: Applied Science and Manufacturing*, 42, 84–91.
- Fowler, P. A., Hughes, J. M., & Elias, R. M. (2006). Biocomposites: Technology, environmental credentials and market forces. *Journal of the Science of Food and Agriculture*, 86, 1781–1789.
- Guo, X., Lin, Y., Na, B., Liang, X., Ekevad, M., Ji, F., & Huang, L. (2016). Evaluation of physical and mechanical properties of fiber-reinforced poplar scrimber. *BioResources*. <https://doi.org/10.15376/biores.12.1.43-55>
- Guo, X., Wang, H., Chen, Q., Na, B., Huang, L., & Xing, F. (2017). The dimensional stability of engineered wood flooring in heating systems. *Wood Res-Slovakia*, 62, 103–111.
- Bai, W., Roy, A., Sun, R., & Silberschmidt, V. V. (2019). Enhanced machinability of SiC-reinforced metal-matrix composite with hybrid turning. *Journal of Materials Processing Technology*, 268, 149–161. <https://doi.org/10.1016/j.jmatprotec.2019.01.017>
- Chawla, N., & Shen, Y. L. (2001). Mechanical behavior of particle reinforced metal matrix composites. *Advanced Engineering Materials*, 3, 357–370.
- Hung, N. P., Boey, F. Y. C., Khor, K. A., Oh, C. A., & Lee, H. F. (1995). Machinability of cast and powder-formed aluminum alloys reinforced with SiC particles. *Journal of Materials Processing Technology*, 48, 291–297. [https://doi.org/10.1016/0924-0136\(94\)01661-J](https://doi.org/10.1016/0924-0136(94)01661-J)
- Yanming, Q., & Zehua, Z. (2000). Tool wear and its mechanism for cutting SiC particle-reinforced aluminium matrix composites. *Journal of Materials Processing Technology*, 100, 194–199. [https://doi.org/10.1016/S0924-0136\(99\)00405-7](https://doi.org/10.1016/S0924-0136(99)00405-7)
- Ding, X., Liew, W. Y. H., & Liu, X. D. (2005). Evaluation of machining performance of MMC with PCBN and PCD tools. *Wear*, 259, 1225–1234.
- Sasimurugan, T., & Palanikumar, K. (2011). Analysis of the machining characteristics on surface roughness of a hybrid aluminium metal matrix composite (Al6061-SiC-Al2O3). *Journal of Minerals and Materials Characterization and Engineering*, 10, 1213–1224. <https://doi.org/10.4236/jmmce.2011.1013094>
- Ge, Y., Xu, J., & Fu, Y. (2011). Experimental study on high-speed milling of SiCp/Al composites. *Materials Processing Technology*, 291, 725.
- Yu, W., Chen, J., Ming, W., An, Q., & Chen, M. (2021). Experimental and FEM study of cutting mechanism and damage behavior of ceramic particles in orthogonal cutting SiCp/Al composites. *Ceramics International*, 47, 7183–7194. <https://doi.org/10.1016/j.ceramint.2020.11.072>
- Bhushan, R. K., Kumar, S., & Das, S. (2010). Effect of machining parameters on surface roughness and tool wear for 7075 Al alloy SiC composite. *The International Journal of Advanced Manufacturing Technology*, 50, 459–469. <https://doi.org/10.1007/s00170-010-2529-2>
- Li, R. R., Xu, W., Wang, X. D., & Wang, C. G. (2018). Modeling and predicting of the color changes of wood surface during CO2 laser modification. *Journal of Cleaner Production*, 183, 818–823.
- Li, W. G., Zhang, Z. K., Peng, X. R., & Li, B. (2017). The influences of circular saws with sawteeth of mic-zero-degree radial clearance angles on surface roughness in wood rip sawing. *Annals of Forest Science*, 74, 1–9.
- Dong, G. J., Zhang, Y. J., Zhou, M., & Wang, Y. J. (2014). The research of effect of cutting parameters on machined surface defects in high-speed milling of SiCp/Al composites. *Key Engineering Materials*, 589, 245. <https://doi.org/10.4028/www.scientific.net/KEM.589-590.245>
- Wang, T., Xie, L. J., Wang, X. B., Jiao, L., Shen, J. W., Xu, H., & Nie, F. M. (2013). Surface integrity of high speed milling of Al/SiC/65p aluminum matrix composites. *Procedia Cirp*, 8, 475–480. <https://doi.org/10.1016/j.procir.2013.06.136>
- Ramanujam, R., Muthukrishnan, N., & Raju, R. (2011). Optimization of cutting parameters for turning Al-SiC(10p) MMC using ANOVA and grey relational analysis. *International Journal of Precision Engineering and Manufacturing*. <https://doi.org/10.1007/s12541-011-0084-x>
- Michalska-Pozoga, I., Tomkowski, R., Rydzkowski, T., & Thakur, V. K. (2016). Towards the usage of image analysis technique to measure particles size and composition in wood-polymer composites. *Industrial Crops and Products*, 92, 149–156. <https://doi.org/10.1016/j.indcrop.2016.08.005>
- Guo, X., Wang, J., Buck, D., Zhu, Z., & Guo, Y. (2021). Machinability of wood fiber/polyethylene composite during orthogonal cutting. *Wood Science and Technology*. <https://doi.org/10.1007/s00226-020-01256-4>

Publisher's Note Springer Nature remains neutral with regard to jurisdictional claims in published maps and institutional affiliations.

Springer Nature or its licensor (e.g. a society or other partner) holds exclusive rights to this article under a publishing agreement with the author(s) or other rightsholder(s); author self-archiving of the accepted manuscript version of this article is solely governed by the terms of such publishing agreement and applicable law.



Jinxin Wang is a Postgraduate student of College Materials Science and Engineering, Nanjing Forestry University, China. His research interests are concerned with cutting technology in composites.



Longzhi Yang received the Ph.D. degree in computer science from University of Wales (Aberystwyth University), Aberystwyth, U.K., in 2011. He is a Professor and Head of Education in the Department of Computer and Information Sciences at Northumbria University, Newcastle upon Tyne, U.K. His research interests include artificial intelligence, machine learning, big data, computer vision, intelligent control systems, and the application of such techniques in real-world uncertain environments.



Rongsheng Jiang got his master degree from Nanjing Forestry University in 2022. During his master's degree, his research interests were concerned with cutting technology in composites and intelligent manufacturing of furniture.

He is the founding Chair of the IEEE Special Interest Group of Big Data for Cyber Security and Privacy, and the Chair of IEEE Computational Intelligence Society Big Data Task Force. Professor Yang is a Senior Member of IEEE and a Senior Fellow of Higher Education Academy of U.K.



Zhanwen Wu is a Postgraduate student of College Materials Science and Engineering, Nanjing Forestry University, China. His research interests are concerned with cutting mechanism and technology.



Pingxiang Cao is a professor of College Materials Science and Engineering, Nanjing Forestry University, China. He is the training target of young and middle-aged academic leaders of “Qinglan Project” in universities of Jiangsu Province, and the leader of scientific and technological innovation training team of “Qinglan Project” in Education Department of Jiangsu Province.



Zhaolong Zhu is a lecturer of College Furnishings and Industrial Design, Nanjing Forestry University, China, and he got his doctoral degree from Nanjing Forestry University in 2020. His research interests are concerned with material machining, digital design and intelligent manufacturing of furniture.